Policy Research Journal
ISSN (E): 3006-7030 ISSN (P) : 3006-7022 Volume 3, Issue 9, 2025

THERMAL DEGRADATION BEHAVIOR AND REACTION KINETICS OF WHEAT HUSK PYROLYSIS

Tarique Ahmed Memon[*1], Faheem Ahmed Solangi[2], Altaf Alam Noonari[3], Sanaullah Mastoi[4], Khudabux Mari[5], Abdul Samad Soomro[6]

[*1]*Department of Mechanical Engineering, The University of Larkano, Sindh, Pakistan.*
[2]*Department of Energy Systems Engineering, Quaid-e-Awam University of Engineering, Science and Technology, Nawabshah, Pakistan.*
[3]*Department of Environmental Sciences, Aror University of Art, Architecture, Design and Heritage, Sukkur, Sindh, Pakistan.*
[4]*Department of Mathematics, The University of Larkano, Sindh, Pakistan.*
[5,6]*Department of Mechanical Engineering Quaid-e-Awam University of Engineering, Science and Technology, Nawabshah, Pakistan.*

[*1]tariquememon@uolrk.edu.pk

DOI: https://doi.org/10.5281/zenodo.17045721

Keywords
Wheat husk; pyrolysis; thermal degradation; kinetics; activation energy

Article History
Received: 11 June 2025
Accepted: 21 August 2025
Published: 03 September 2025

Copyright @Author

Corresponding Author: *
Tarique Ahmed Memon

Abstract

This study investigated the pyrolysis behavior and reaction kinetics of wheat husk (WH) using thermogravimetric analyzer (TGA) at heating rates of 10, 20, 30, 40, and 50 °C/min from ambient temperature to 850 °C. TGA profiles revealed that the most significant weight loss occurred within the major devolatilization region. A systematic increase in the peak temperature (T_{max}), the maximum devolatilization rate (W_{max}), and the final solid residue (SR) was observed with increasing higher heating rate. Kinetic analysis, performed using the Friedman and FWO methods., yielded activation energy (E_a) values that remained nearly constant until α=0.7, beyond which a pronounced increase was observed. The calculated E_a values ranged from 115.71 to 378.66 kJ/mol (Friedman), and 129.01 to 344.38 kJ/mol (FWO), with coefficient of determination (R^2 >0.96) for both methods validate the reliability of E_a calculations. The master plot technique identified the F3 reaction model as the most suitable mechanism for describing the pyrolysis process. Finally, the pre-exponential factor (A) values ranged from 2.44×10^9 to 2.11×10^{26} s^{-1}.

1. INTRODUCTION

The increasing global population and economic growth have resulted in a rapid rise in energy demand. This demand is predominantly met by fossil fuels (coal, oil, natural gas), which account for over 80% of the global energy mix [1]. The combustion of these fuels across various factors such as transportation, power generation, and industry is the primary driver of persistently rising CO_2 emissions, posing a significant threat to both environmental stability and human health [2]. In response, biomass

has emerged as a crucial renewable energy alternative to fossil fuels [3]. Thermochemical conversion technologies, particularly pyrolysis, present a viable pathway for transforming biomass waste into valuable products, thereby mitigating environmental impacts and enhancing resource efficiency [4]. To analyze these conversion processes, thermogravimetric analysis (TGA) is employed. This technique measures a sample's mass change as a function of time or temperature to characterize its thermal degradation, and determine key kinetic parameters, including activation energy (E_a), pre-exponential factor (A), and the kinetic model [5]. Numerious studies have investigated the thermochemical conversion of various agricultural waste. Hýsek et al. [6] studied the effect of wheat husk on the properties of the particle and composite materials. Rajkumar and Murugavelh [7] conducted the co-pyrolysis of wheat husk and residual tyre in a fixed bed reactor. Lanzetta and Blasi [8] investigated the pyrolysis of wheat straw and corn stalks. Similarly, Mansoor et al. [9] explored the potential of corn husk through pyrolysis and gasification, conducting a detailed kinetic and thermodynamic analysis. Dammu et al. [10] performed a thermo-kinetic analysis of onion peels, while Jarrahi et al. [11] utilized wheat straw and wheat husk to create rGO aerogels for photothermal materials in solar evaporation systems. Mona et al. [12] produced biochar from wheat husk and algal biomass for soil amendment to improve fertility. Neitzel et al. [13] investigated wheat, barley, and oat husks as alternative raw materials for particleboard manufacturing. The thermo-kinetic behavior of various agricultural residues has been extensively investigated using TGA. For instance, banana leaves [14], mango seeds [15], and a variety of fruit and vegetable peels, including papaya, pineapple, potato, and lettuce [16]. However, a review of the literature indicates that studies specifically investigating the thermal degradation and pyrolysis kinetics of wheat husk remain scarce.

This study investigated the pyrolysis behavior of wheat husk using thermogravimetric analyzer at heating rates of 10, 20, 30, 40, and 50 °C/min from ambient temperature to 850 °C. The kinetic triplet including activation energy (E_a), pre-exponential factor (A), and the kinetic model was determined using the Friedman, FWO methods along with the master plot technique.

Materials and Methods

Samples preparation

Wheat husk (WH) was obtained from a local flour mill in Therhi, District Khairpur Mirs, Pakistan. The raw biomass was sun-dried for seven days to reduce initial moisture content, then ground and sieved to a uniform particle size of 0.20 mm. Finally, the sieved samples were stored in airtight containers to prevent moisture absorption from the atmosphere.

Pyrolysis experiments

The pyrolysis behavior of the wheat husk (WH) sample was investigated using thermogravimetric analysis (TGA). For each experiment, approximately 10 mg of sample was loaded in a crucible. An inert atmosphere was maintained by purging pure nitrogen at a constant flow rate of 50 mL/min. First, the sample was heated from ambient temperature to 150 °C to eliminate residual moisture. Subsequently, the temperature was increased to 850 °C at five heating rates (10, 20, 30, 40, and 50 °C/min) to study the pyrolysis.

Kinetic modelling

The kinetic analysis of the solid-state pyrolysis reaction is based on the extent of conversion (α) is mathematically expressed as:

$$\alpha = \frac{xi - xt}{xi - xf} \qquad (1)$$

where, x_i is the initial sample mass, x_t is mass at time t, and x_f is final residual mass after the reaction is complete.

The rate of a solid-state reaction is commonly described by the following equation:

$$\frac{d\alpha}{dt} = A \exp\left(-\frac{Ea}{RT}\right) f(\alpha) \qquad (2)$$

where t is the time, A is the pre-exponential factor, E_a is the activation energy, R is the universal gas constant, T is the temperature, and $f(\alpha)$ is the kinetic model.

Equation (2) can be rearranged by substituting $dt = dT/\beta$ to give:

$$\frac{d\alpha}{f(\alpha)} = \frac{A}{\beta} \exp\left(-\frac{Ea}{RT}\right) dT \qquad (3)$$

Where β is the heating rate. The integral form of Eq. (3) can be written in the following equation:

$$g(\alpha) = \int_0^{\alpha} \frac{d\alpha}{f(\alpha)} = \frac{A}{\beta} \int_{To}^{T} \exp(-\frac{Ea}{RT}) dT \quad (4)$$

Where, T_o is the initial temperature.

Friedman method

$$\ln\left(\frac{da}{dt}\right) = \ln[Af(a)] - \frac{Ea}{RT} \quad (5)$$

Flynn-Wall-Ozawa (FWO) method [17]

$$\ln(\beta) = \ln\left[\frac{AE_a}{RG(\alpha)}\right] - 5.331 - 1.052\left(\frac{E_a}{RT}\right) \quad (6)$$

The kinetic parameters were determined by constructing linear plots according to the Friedman and FWO methods. For a given conversion (α), the Friedman method was applied by plotting $\ln\left(\frac{da}{dt}\right)$ versus 1000/T, while the FWO method was applied by plotting ln(β) versus 1000/T. In both cases, the activation energy (E_a) was calculated from the slope of the resulting linear fit.

The master plot method was employed to determine the pyrolysis reaction mechanism. This approach utilizes the fundamental relationship expressed in Eq. (4) [18]:

$$g(\alpha) = \frac{AE_a}{\beta R} p(u) \quad (7)$$

where $u = E_a/RT$. Here, $p(u)$ is approximated as follows [19].

$$p(u) = \frac{\exp(-u)}{u \times (1.00198882u + 1.87391198)} \quad (8)$$

The normalized form of Eq. (7) at α=0.5 is written as follows [20]:

$$z(\alpha) = \frac{g(\alpha)}{g(0.5)} = \frac{p(u)}{p(u_{0.5})} \quad (9)$$

The most probable reaction mechanism was determined by comparing the theoretical master plots of $g(\alpha)/g(0.5)$ with the experimental curves of $p(u)/p(0.5)$. The common reaction mechanisms considered in this work are summarized in Table 1.

Table 1 Solid-state kinetic models for pyrolysis [21][22]

Types	Representation	$f(\alpha)$	$g(\alpha)$
Diffusion	D1	$1/(2\alpha)$	α^2
	D2	$[-\ln(1-\alpha)]^{-1}$	$(1-\alpha)\ln(1-\alpha)+\alpha$
	D3	$3/2(1-\alpha)^{2/3}[1-(1-\alpha)^{1/3}]^{-1}$	$[1-(1-\alpha)^{1/3}]^2$
Order based	F_n	$(1-\alpha)^n$	$1/(n-1)[(1-\alpha)^{(1-n)}-1]$
Power law	P2	$2\,\alpha^{1/2}$	$\alpha^{1/2}$
	P3	$3\,\alpha^{2/3}$	$\alpha^{1/3}$
Geometrical contraction models	R1	1	α
	R2	$2\,(1-\alpha)^{1/2}$	$1-(1-\alpha)^{1/2}$

Results and Discussions

Pyrolysis experiments

Figure 1 illustrates the thermogravimetric (TG) and derivative thermogravimetric (DTG) curves for wheat husk (WH) pyrolysis, conducted from room temperature to 850 °C at heating rates of 10, 20, 30, 40, and 50 °C/min. The thermal degradation can be divided into three distinct stages. The initial stage occurring between ambient temperature and 150 °C, is attributed to the dehydration of the sample, involving the removal of physically absorbed moisture. The second stage (150-600 °C) represents the active pyrolysis zone, where the devolatilization of hemicellulose and cellulose takes place, resulting in the maximum rate of mass loss. The corresponding DTG curve for this region is characterized by a distinct shoulder followed by a sharper peak. These features are assigned to the decomposition of hemicellulose and cellulose, respectively, which occur concurrently with the slower degradation of lignin [23]. The final stage (600-850 °C) involves slow char formation dominates with minimal mass loss due to slow decomposition of remaining lignin.

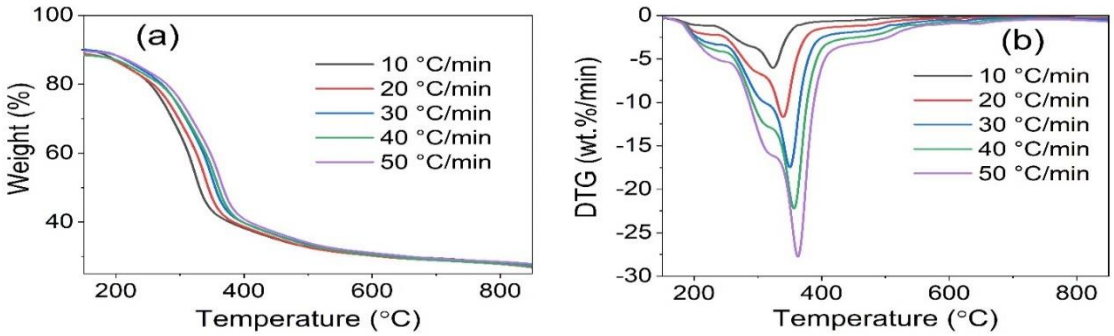


Figure 1. TG/DTG curves for biomass pyrolysis at various heating rate

The key pyrolysis parameters derived from the TG/DTG curves at each heating rate are summarized in Table 2. As expected, the most significant weight loss occurred within the major devolatilization region (150 to 600 °C). A clear dependence on heating rate was observed for several parameters. Both the peak temperature (T_{max}) and the corresponding maximum devolatilization rate (W_{max}) exhibited a systematic increase as the heating rate was elevated. The T_{max} and W_{max} increased with increasing heating rate. Similarly, the yield of solid residue (SR) at the final temperature was also found to increase with higher heating rates.

Table 2. Influence of heating rates on pyrolysis characteristics of biomass

H.R (°C/min)	Weight loss (%)	T_{max} (°C)	W_{max} (wt.%/min)	SR (%)
10	59.24	324.03	6.04	26.86
20	58.42	340.05	11.68	26.98
30	59.25	351.95	17.31	27.63
40	57.87	357.66	22.13	27.25
50	58.48	363.80	27.66	27.89

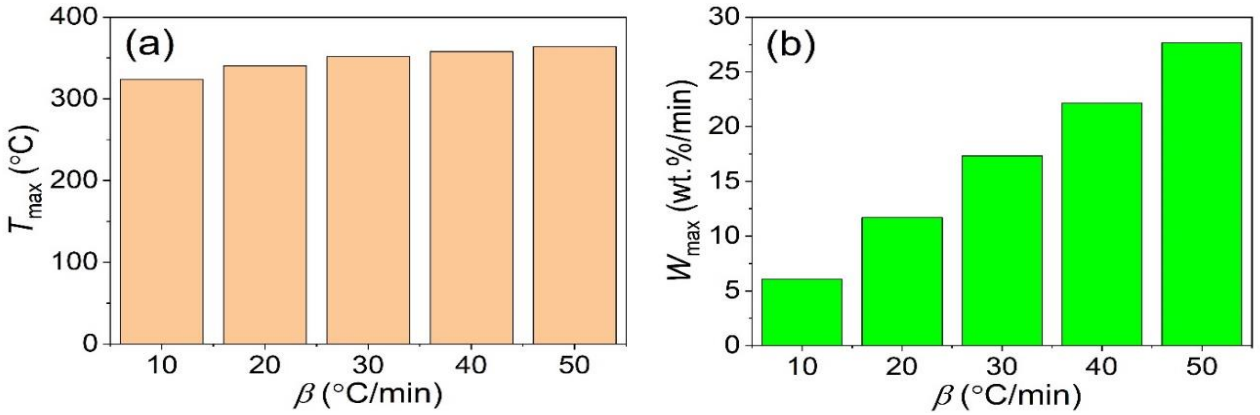


Figure 2. Influence of various heating rates on: (a) T_{max} and (b) W_{max}.

Kinetic analysis

The kinetic parameters comprising activation energy (E_a), pre-exponential factor (A), were calculated using two isoconversional methods, such as Friedman and FWO methods. Thermogravimetric analysis was conducted at heating rates of 10, 20, 30, 40 and 50 °C/min to investigate their effect on thermal degradation. The resulting mass loss data were used to calculate the conversion rate (α) as a function of temperature for each heating rate. For each α value, the left-hand side of the kinetic equation was plotted against the inverse temperature. For a given conversion (α), the Friedman method was applied by plotting $\ln\left(\frac{da}{dt}\right)$ versus $1000/T$, while the FWO method was applied by plotting $\ln(\beta)$ versus $1000/T$. The scatter plots were subjected to linear regression, as shown in Figure 3. The E_a for each α value was then calculated from the slope of the respective regression lines.

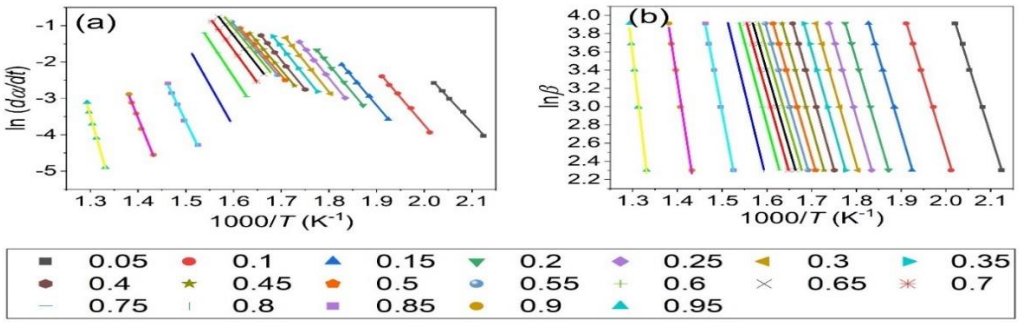


Figure 3. Linear fitting plots for activation energy using (a) Friedman, and (b) FWO methods.

Figure 4 illustrates the variation in E_a and conversion (α) during pyrolysis, as determined by the Friedman and FWO methods. For the biomass sample, the E_a values from both methods remained nearly constant until α=0.7. Beyond this point, a pronounced rise in E_a was observed, continuing until the conversion was complete. The lower E_a-values observed at the initial stage are likely attributed to the decomposition of hemicellulose and cellulose. The later stage is attributed to the more thermally stable and complex structure of lignin, which requires a higher energy barrier for its decomposition. The calculated E_a values ranged from 115.71 to 378.66 kJ/mol for the Friedman method, and 129.01 to 344.38 kJ/mol for the FWO method. The coefficient of determination (R^2) was greater than 0.96 for both methods, indicating a strong correlation between the experimental data and the kinetic model.

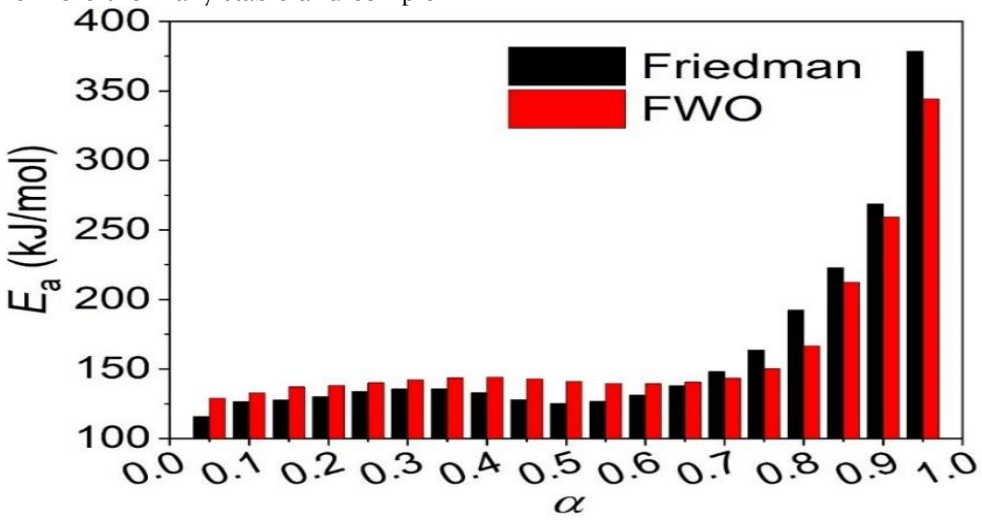


Figure 4. E_a variation with conversion using Friedman and FWO methods.

The master plot technique was employed to identify the mechanism governing the thermal degradation of the sample. Using the E_a values and temperature data at various conversion levels. The experimental $p(u)$ function was determined. Experimental plots of $p(u)/p(u0.5)$ versus α, generated at heating rates of 10, 20, 30, and 40, and 50 °C/min, exhibited nearly identical behavior, indicating that the degradation mechanism is independent of heating rate [24]. These experimental curves were then compared to theoretical master plots, $g(\alpha)/g(0.5)$, representing various reaction mechanisms as shown in Figure 5. For WH, the experimental plot showed a close match with the F3 model, suggesting that the pyrolysis process is best described by a third order reaction mechanism.

Additionally, the pre-exponential factor (A) was determined, with calculated A values ranging from 2.44×10^{9} to 2.11×10^{26} s^{-1}. The observed increase in A with conversion suggests a greater frequency of molecular collisions as the degradation process advances.

Furthermore, the compensation effect was investigated. As depicted in Figure 6, a strong linear relationship exists between the activation energy (E_a) and the natural logarithm of pre-exponential factor (ln$A$) for the data obtained from the both Friedman and FWO methods.

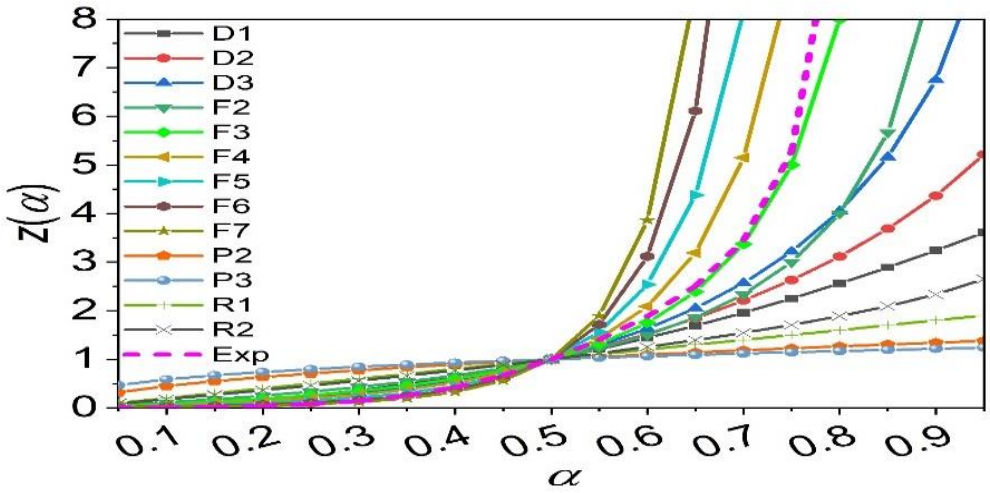


Figure 5. Comparison of experimental and theoretical master plot curves.

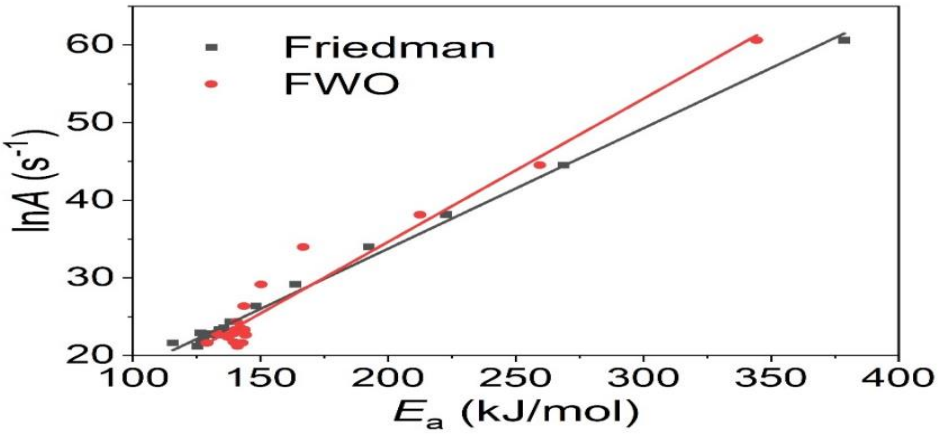


Figure 6. Relationship between E_a and ln$A$ obtained by Friedman and FWO methods.

Conclusions

This study investigated the pyrolysis behavior of wheat husk (WH) using thermogravimetric analyzer at heating rates of 10, 20, 30, 40, and 50 °C/min from ambient temperature to 850 °C. The pyrolysis behavior of WH sample was investigated using thermogravimetric analysis (TGA). During thermogravimetric analysis, the most significant weight loss occurred within the major devolatilization region. Both the peak temperature (T_{max}) and the corresponding maximum devolatilization rate (W_{max}) exhibited a systematic increase as the heating rate was elevated. Similarly, the yield of solid residue (SR) at the final temperature was also found to increase with higher heating rates. The kinetic analysis was conducted using two isoconversional methods, such as Friedman and FWO. The E_a values from both methods remained nearly constant until α=0.7. Beyond this point, a pronounced rise in E_a was observed, continuing until the conversion was complete. The calculated E_a values ranged from 115.71 to 378.66 kJ/mol for the Friedman method, and 129.01 to 344.38 kJ/mol for the FWO method. The coefficient of determination (R^2) was greater than 0.96 for both methods, indicating a strong correlation between the experimental data and the kinetic model. The master plot technique was employed to identify the mechanism governing the thermal degradation of the sample, the experimental plot showed a close match with the F3 model, suggesting that the pyrolysis process is best described by a third order reaction mechanism. Additionally, the pre-exponential factor (A) values ranging from 2.44×10^{9} to 2.11×10^{26} s^{-1}.

REFERENCES

1. Sundaram T, Kamalesh R, Saravanan A, et al (2025) International Journal of Biological Macromolecules Harnessing algal biomass for renewable energy and biofuel production : Current strategies and future insights ☆. Int J Biol Macromol 319:145487. https://doi.org/10.1016/j.ijbiomac.2025.145487
2. Zhao J, Dong K, Dong X, Shahbaz M (2022) How renewable energy alleviate energy poverty? A global analysis. Renew Energy 186:299–311. https://doi.org/10.1016/J.RENENE.2022.01.005
3. Jonathan AE, Agbajor GK, David OO, et al (2025) Determination and prediction of biogas production potential from selected biomasses as alternative renewable energy source in Sapele , Nigeria. Renew Energy 255:123802. https://doi.org/10.1016/j.renene.2025.123802
4. Promraksa A, Seekao N, Mueanmas C, et al (2025) Synergistic Co-Pyrolysis of biomass for renewable energy: Enhanced energy recovery and heat integration from non-condensable gases. Energy Convers Manag 343:. https://doi.org/10.1016/j.enconman.2025.120260
5. Solís RR, Bl G (2025) Thermogravimetric analysis of textile waste : kinetic parameters and pyrolytic decomposition mechanisms. 65:. https://doi.org/10.1016/j.tsep.2025.103946
6. Hýsek Š, Podlena M, Bartsch H, et al (2018) Effect of wheat husk surface pre-treatment on the properties of husk-based composite materials. Ind Crops Prod 125:105–113. https://doi.org/10.1016/J.INDCROP.2018.08.035
7. Rajkumar P, Murugavelh S (2022) (a) (b). Bioresour Technol Reports 19:101164. https://doi.org/10.1016/j.biteb.2022.101164
8. Lanzetta M, Di Blasi C (1998) Pyrolysis kinetics of wheat and corn straw. J Anal Appl Pyrolysis 44:181–192. https://doi.org/10.1016/S0165-2370(97)00079-X

9. Lu Z, Li K, Yang J, et al (2024) Unlocking the Full Potential of Green Catalysis: a Novel Thermosensitive Catalytic System for Ultrasonic-microwave Liquefaction of Woody Biomass. Ind Crops Prod 215:. https://doi.org/10.1016/j.indcrop.2024.118678
10. Dammu AK, Nisa S, Shergujri MA, Bhaduri GA (2025) Chemical Engineering Research and Design Pyrolysis of onion peel waste : Effect of extraction on kinetics and thermodynamics for a sustainable bioeconomy. Chem Eng Res Des 219:414–428. https://doi.org/10.1016/j.cherd.2025.06.016
11. Jarrahi Z, Mehmandoost M, Choobdari M, et al (2025) Impact of wheat husk / wheat straw loading ratio on solar evaporation performance of cost-effective sustainable rGO-based hybrid aerogels. Surfaces and Interfaces 72:107294. https://doi.org/10.1016/j.surfin.2025.107294
12. Mona S, Saini N, Kumar S, et al (2024) Bioresource Technology Reports Characterization and utilization of algal and wheat husk biochar as biofertilizers for sustainable soil amelioration. Bioresour Technol Reports 27:101893. https://doi.org/10.1016/j.biteb.2024.101893
13. Neitzel N, Eder M, Hosseinpourpia R, et al (2023) Chemical composition , particle geometry , and micro-mechanical strength of barley husks , oat husks , and wheat bran as alternative raw materials for particleboards. Mater Today Commun 36:106602. https://doi.org/10.1016/j.mtcomm.2023.106602
14. Priyadarsini A, Swain B, Mishra A, et al (2023) Study on biofuel efficiency of tropical banana leaf biomass using spectroscopy, kinetic and thermodynamic parameters. Bioresour Technol Reports 23:101522. https://doi.org/10.1016/j.biteb.2023.101522
15. Alves JLF, da Silva JCG, Mumbach GD, et al (2023) Physicochemical properties, pyrolysis kinetics, thermodynamic parameters of activation, and evolved volatiles of mango seed waste as a bioenergy feedstock: A potential exploration. Thermochim Acta 725:. https://doi.org/10.1016/j.tca.2023.179519
16. Pardo RNC, Rojas GMA, Florez LM (2023) Thermal analysis of the physicochemical properties of organic waste to application in the compost process. Biomass Convers Biorefinery 13:7097–7109. https://doi.org/10.1007/s13399-021-01786-2
17. Al-Balushi FA, Burra KG, Chai Y, Wang M (2023) Co-pyrolysis of waste tyre and pine bark: Study of reaction kinetics and mechanisms. Biomass and Bioenergy 168:106654. https://doi.org/10.1016/j.biombioe.2022.106654
18. Cai H, Liu J, Xie W, et al (2019) Pyrolytic kinetics, reaction mechanisms and products of waste tea via TG-FTIR and Py-GC/MS. Energy Convers Manag 184:436–447. https://doi.org/10.1016/j.enconman.2019.01.031
19. Chen J, Mu L, Jiang B, et al (2015) TG/DSC-FTIR and Py-GC investigation on pyrolysis characteristics of petrochemical wastewater sludge. Bioresour Technol 192:1–10. https://doi.org/10.1016/j.biortech.2015.05.031
20. Vyazovkin S, Burnham AK, Criado JM, et al (2011) Thermochimica Acta ICTAC Kinetics Committee recommendations for performing kinetic computations on thermal analysis data. Thermochim Acta 520:1–19. https://doi.org/10.1016/j.tca.2011.03.034

21. Ma C, Zhang F, Hu J, et al (2023) Bioresource Technology Co-pyrolysis of sewage sludge and waste tobacco stem : Gas products analysis , pyrolysis kinetics , artificial neural network modeling , and synergistic effects. Bioresour Technol 389:129816. https://doi.org/10.1016/j.biortech.2023.129816

22. Alves JLF, da Silva JCG, da Silva Filho VF, et al (2019) Kinetics and thermodynamics parameters evaluation of pyrolysis of invasive aquatic macrophytes to determine their bioenergy potentials. Biomass and Bioenergy 121:28–40. https://doi.org/10.1016/j.biombioe.2018.12.015

23. Lei J, Ye X, Wang H, Zhao D (2023) Insights into Pyrolysis Kinetics , Thermodynamics , and the Reaction Mechanism of Wheat Straw for Its Resource Utilization

24. Ghadikolaei SS, Omrani A, Ehsani M (2017) Non-isothermal degradation kinetics of Ethylene-Vinyl Acetate Copolymer nanocomposite reinforced with modified Bacterial Cellulose Nanofibers using advanced isoconversional and master plot analyses. Thermochim Acta 655:87–93. https://doi.org/10.1016/j.tca.2017.06.014

IEER
Institute for Excellence in Education & Research